The $\beta G^{156}C$ Substitution in the F_1-ATPase from the Thermophilic *Bacillus* PS3 Affects Catalytic Site Cooperativity by Destabilizing the Closed Conformation of the Catalytic Site†

Sanjay Bandyopadhyay, Carolina R. Valder, Hue G. Huynh, Huimiao Ren, and William S. Allison*

Department of Chemistry & Biochemistry, University of California at San Diego, La Jolla, California 92093-0601

Received June 4, 2002; Revised Manuscript Received September 27, 2002

ABSTRACT: Fluorescence titrations of the $\alpha_3(\beta G^{156}C/Y^{345}W)_3\gamma$, $\alpha_3(\beta E^{199}V/Y^{345}W)_3\gamma$, and $\alpha_3(\beta Y^{345}W)_3\gamma$ subcomplexes of TF_1 with nucleotides show that the $\beta G^{156}C$ substitution substantially lowers the affinity of catalytic sites for ATP and ADP with or without Mg^{2+}, whereas the $\beta E^{199}V$ substitution increases the affinity of catalytic sites for nucleotides. Whereas the $\alpha_3(\beta G^{156}C)_3\gamma$ and $\alpha_3(\beta E^{199}V)_3\gamma$ subcomplexes hydrolyze 2 mM ATP at 2% and 0.7%, respectively, of the rate exhibited by the wild-type enzyme, the $\alpha_3(\beta G^{156}C/E^{199}V)_3\gamma$ hydrolyzes 2 mM ATP at 9% the rate exhibited by the wild-type enzyme. The $\alpha_3(\beta G^{156}C)_3\gamma$, $\alpha_3(\beta G^{156}C/E^{199}V)_3\gamma$, and $\alpha_3(\beta G^{156}C/E^{199}V/Y^{345}W)_3\gamma$ subcomplexes resist entrapment of inhibitory MgADP in a catalytic site during turnover. Product [^{3}H]ADP remains tightly bound to a single catalytic site when the wild-type, $\beta E^{199}V$, $\beta Y^{345}W$, and $\beta E^{199}V/Y^{345}W$ subcomplexes hydrolyze substoichiometric [^{3}H]ATP, whereas it is not retained by the $\beta G^{156}C$ and $\beta G^{156}C/Y^{345}W$ subcomplexes. Less firmly bound, product [^{3}H]ADP is retained when the $\beta G^{156}C/E^{199}V$ and $\beta G^{156}C/E^{199}V/Y^{345}W$ mutants hydrolyze substoichiometric [^{3}H]ATP. The Lineweaver−Burk plot obtained with the $\beta G^{156}C$ mutant is curved downward in a manner indicating that its catalytic sites act independently during ATP hydrolysis. In contrast, the $\beta G^{156}C/E^{199}V$ and $\beta G^{156}C/E^{199}V/Y^{345}W$ mutants hydrolyze ATP with linear Lineweaver−Burk plots, indicating cooperative trisite catalysis. It appears that the $\beta G^{156}C$ substitution destabilizes the closed conformation of a catalytic site hydrolyzing MgATP in a manner that allows release of products in the absence of catalytic site cooperativity. Insertion of the $\beta E^{199}V$ substitution into the $\beta G^{156}C$ mutant restores cooperativity by restricting opening of the catalytic site hydrolyzing MgATP for product release until an open catalytic site binds MgATP.

The F_1 component of the F_oF_1-ATP synthases found in energy-transducing membranes contains the catalytic sites for ATP synthesis. When removed from the membrane, F_1 is an ATPase comprised of five subunits in $\alpha_3\beta_3\gamma\delta\epsilon$ stoichiometry (*1*, *2*). Isolated F_1-ATPases contain six binding sites for adenine nucleotides. Three of these are catalytic sites that are located mostly on β subunits. The other three, the physiological function of which is unknown, are located mostly on α subunits and are called noncatalytic nucleotide binding sites.

In the original crystal structure of bovine MF_1[1,2] deduced by Abrahams et al. (*3*), the α and β subunits are elongated in an alternating, hexameric array that surrounds a coiled coil made up of the α-helical N- and C-termini of the γ subunit. In this and other crystal structures of bovine MF_1 (*4*−*6*), noncatalytic sites are homogeneously liganded with MgAMP-PNP and α subunits are present in closed conformations, whereas catalytic sites are heterogeneously liganded. In the original crystal structure, two β subunits are in closed conformations. One, designated β_T, contains MgAMP-PNP bound to the catalytic site, and another, designated β_D, contains MgADP bound to the catalytic site. The third β subunit, designated β_E, is in an open conformation with an empty catalytic site (*3*). Amino acid side chains that interact with anionic oxygens of nucleotides or the Mg^{2+} ion complexed with anionic oxygens of bound nucleotides are arranged similarly in catalytic sites of β_T and β_D that have closed conformations, but are arranged very differently in the catalytic site of β_E that has an open conformation.

Consistent with the predictions based on Boyer's binding change mechanism (*1*), single-molecule experiments pioneered by the collaborative efforts of the Yoshida and Kinosita laboratories have shown that sequential firing of the three catalytic sites of F_1 during ATP hydrolysis is coupled to counterclockwise rotation of the γ subunit that occurs in distinct steps (*7*−*9*).

ATP hydrolysis by isolated F_1-ATPases is inhibited when a single catalytic site contains tightly bound MgADP. The

† This work was supported by NIGMS Grant GM 16974 from the National Institutes of Health. C.R.V. was supported by an award from the Ronald E. McNair Achievement Program funded by the U.S. Department of Education.

* To whom correspondence should be addressed. Phone: (858) 534-3057. Fax: (858) 822-0079. E-mail: wsa@checfs2.ucsd.edu.

[1] Abbreviations: MF_1, TF_1, EF_1, the F_1-ATPases from bovine heart mitochondria, the thermophilic *Bacillus* PS3, and *Escherichia coli*, respectively; AMP-PNP, 5′-adenylyl β,γ-imidophosphate; LDAO, lauryl dimethylamine oxide.

[2] Residue numbers of MF_1 are used throughout. In MF_1, βG^{156} is equivalent to βG^{158} of TF_1 and βG^{149} of EF_1, βE^{199} of MF_1 is equivalent to βE^{201} of TF_1 and βE^{192} of EF_1, βY^{345} in MF_1 is equivalent to βY^{341} of TF_1 and βY^{331} of EF_1, and βF^{155} in MF_1 is equivalent to βF^{157} in TF_1.

10.1021/bi026243g CCC: $22.00
Published on Web 11/08/2002

single catalytic site can be loaded by adding stoichiometric MgADP or by adding stoichiometric MgATP that is then hydrolyzed (*10*−*13*). Transient entrapment of inhibitory MgADP in a catalytic site occurs in a turnover-dependent manner when F_1-ATPases hydrolyze ATP even in the presence of a substrate regeneration system, especially when noncatalytic sites are not saturated with ATP (*14*−*17*). For instance, nucleotide-depleted MF_1, TF_1, and the $\alpha_3\beta_3\gamma$ subcomplex of TF_1 hydrolyze 50 μM ATP in three distinct kinetic phases in the presence of an ATP regenerating system. An initial burst of hydrolysis rapidly decelerates to a slower rate, which in turn slowly accelerates to a faster rate approaching the initial rate. Transition from the burst phase to the slow intermediate phase is caused by entrapment of inhibitory MgADP in a catalytic site. Slow binding of ATP to noncatalytic sites is responsible for transition from the slow intermediate phase to the final rate (*15*). Turnover-dependent entrapment of inhibitory MgADP is provoked by azide, presumably because it stabilizes MgADP complexed with the single catalytic site (*18*). In the case of MF_1, saturation of noncatalytic sites with $MgPP_i$ prevents entrapment of inhibitory MgADP during turnover (*19*, *20*). Turnover-dependent entrapment of inhibitory MgADP by TF_1 and its $\alpha_3\beta_3\gamma$ subcomplex is relieved by the nonionic detergent LDAO (*16*, *17*).

A previous study showed that the $\beta E^{199}C$ and $\beta E^{199}V$ substitutions in the $\alpha_3\beta_3\gamma$ subcomplex of TF_1 decreased k_{cat} 20-fold and 60-fold, respectively, and decreased K_m 50-fold and 10-fold, respectively (*21*). Moreover, each mutant enzyme was more sensitive to inhibition by azide than the wild type. Given that, in crystal structures, the hydroxyl oxygen of βThr^{163} interacts directly with Mg^{2+} complexed with MgADP and MgAMP-PNP, in β_T and β_D, respectively, whereas in β_E, the hydroxyl is H-bonded to the carboxylate of βGlu^{199} (*3*−*6*), it was proposed that substitution of βGlu^{199} with Cys or Val increased the affinity of catalytic sites for nucleotides by destabilizing the open conformation of the catalytic site. Subsequently, it was recognized from an earlier report by Iwamoto et al. (*22*) that the $\beta E^{199}V$ substitution in *Escherichia coli* F_1 suppressed the effects of the $\beta G^{156}C$ mutation. They showed that an *E. coli* strain carrying the $\beta G^{156}C/E^{199}V$ double mutation grows on succinate, whereas a strain carrying the $\beta G^{156}C$ single mutation does not. This suggested that the strain with the $\beta G^{156}C$ single substitution causes defective oxidative phosphorylation.

Gly^{156} is the first amino acid in a six-residue Ω-loop (*23*) with the sequence $^{156}GGAGVG^{161}$ in the nucleotide-binding domain of β subunits, which connects β-strand 3 and α-helix B with a reversed turn. In crystal structures of MF_1, oxygens of β-phosphates of nucleotides bound to catalytic sites appear to H-bond to amide hydrogens of βGly^{159} and βGly^{161} in the Ω-loop. The aim of this study was to determine whether the $\beta G^{156}C$ substitution alters ATP hydrolysis by lowering the affinity of catalytic sites for ATP. To accomplish this, the catalytic properties of the $\beta G^{156}C$ and $\beta E^{199}V$ single mutants, $\beta G^{156}C/\beta E^{199}V$ double mutant, and wild-type enzymes have been compared. Moreover, the affinities of catalytic sites for nucleotides in the $\beta G^{156}C/Y^{345}W$ and $\beta E^{199}V/Y^{345}W$ double mutants and $\beta G^{156}C/E^{199}V/Y^{345}W$ triple mutant have been compared with the affinities of catalytic sites in the $\beta Y^{345}W$ single mutant by fluorescence titrations of the introduced tryptophans with nucleotides.

EXPERIMENTAL PROCEDURES

Construction of the Mutant Plasmids. Plasmid pKK, which carries the genes encoding the α, β, and γ subunits of TF_1, was used for both site-directed mutagenesis and gene expression (*24*). Expression plasmids were constructed using the polymerase chain reaction and the QuikChange site-directed mutagenesis kit (Stratagene). The plasmids were purified using the Wizard Plus miniprep kit (Promega). The $\beta G^{156}C$ single mutant was generated with the mutagenic oligonucleotide 5′-CGGTTTGTTC*TGC*GGCGCTGGCG-TAGG-3′ and its corresponding complement (not shown) using wild-type pKK as template. The bases changed are italic. The $\beta Y^{345}W$ (*25*) single mutant plasmid DNA was used as a template to generate the $\beta E^{199}V/Y^{345}W$ double mutant. The $\beta Y^{345}W$ and $\beta E^{199}V$ (*21*) mutant plasmids were used as templates to generate the $\beta G^{156}C/Y^{345}W$ and $\beta G^{156}C/E^{199}V$ double mutants, respectively. The $\beta G^{156}C/E^{199}V$ double mutant plasmid DNA was used as a template to generate the $\beta G^{156}C/E^{199}V/Y^{345}W$ triple mutant. After mutations were confirmed by sequence analysis, the mutant pKK plasmids were expressed in *E. coli* strain JM103 (*unc*$^-$). The wild-type and mutant subcomplexes were purified as described previously and stored as suspensions in 75% saturated ammonium sulfate at 4 °C (*24*).

Removal of Endogenous Nucleotides from the Isolated Wild-Type and Mutant Subcomplexes. Unless stated otherwise, solutions of the enzyme were prepared by dissolving pelleted ammonium sulfate precipitates obtained by centrifugation in 50 mM Tris−Cl, pH 8.0, containing 10 mM CDTA. After 30 min at 23 °C, 100 μL aliquots of the solutions were passed through 1 mL centrifuge columns of Sephadex G-50 (*26*) equilibrated with 50 mM Tris−Cl, pH 8.0, containing 0.1 mM EDTA. Protein concentrations were determined with Coomassie Blue (Pierce) by the method of Bradford (*27*). Endogenous nucleotides bound to the enzyme subcomplexes were determined by HPLC on a TSK-DEAE-5PW Sepherogel column equilibrated and eluted with 50 mM KH_2PO_4, pH 4.3, containing 120 mM NaCl. The CDTA-treated wild-type and mutant subcomplexes were essentially free of endogenous nucleotide.

Assays of ATP Hydrolysis under Single-Site and Multiple-Site Conditions. Hydrolysis of ATP under single-site conditions was performed at 23 °C by rapidly mixing a substoichiometric amount of [^{3}H]ATP (1.7 μM final concentration) with 2.85 μM (1 mg/mL) wild-type or mutant subcomplex in 50 mM Tris−Cl, pH 8.0, containing 1 mM $MgCl_2$. To determine the rate of ATP hydrolysis, 2 μL of 60% perchloric acid was added to 75 μL samples of the reaction mixtures in 0.5 mL centrifuge tubes that were withdrawn at increasing time intervals. After 10 min, perchloric acid was neutralized by addition of 2 μL of 9.2 M KOH and the samples were placed on ice for 10 min before precipitated $KClO_4$ and denatured protein were removed by centrifugation. The quantity of [^{3}H]ADP in the supernatants was determined by anion exchange HPLC to estimate the extent of hydrolysis of the [^{3}H]ATP added to the subcomplexes. The amount of product [^{3}H]ADP remaining bound to the enzyme subcomplexes was determined by passing 75 μL samples of reaction mixtures through 1 mL centrifuge columns of Sephadex G-50 equilibrated with 50 mM Tris−Cl, pH 8.0, at increasing time intervals into centrifuge tubes containing 2 μL of 60%

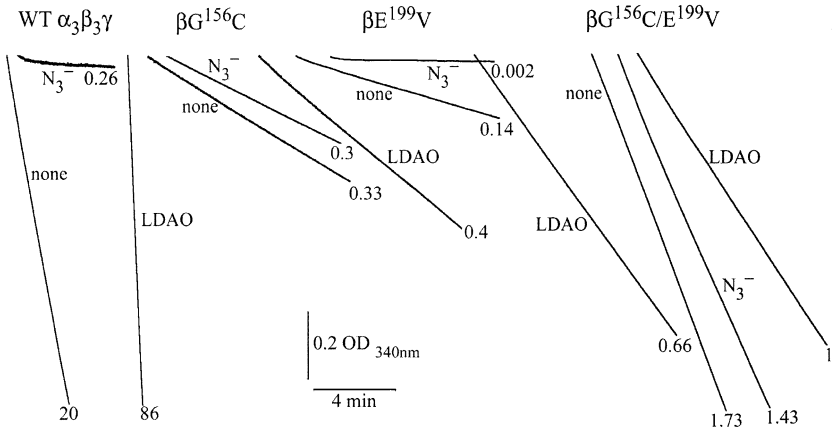

FIGURE 1: Comparison of the effects of NaN_3 and LDAO on the hydrolysis of ATP by the wild-type and mutant enzyme subcomplexes. Hydrolysis of 2 mM ATP was carried out using an ATP regenerating system (*15*) in the presence of 3 mM Mg^{2+} at 30 °C. Assays were initiated by injecting 2 μg of the wild type and 15 μg each of the mutant enzyme subcomplexes into 1 mL of assay medium in the presence or absence of 1 mM NaN_3 or 0.06% LDAO, as specified. The numbers on the traces represent the final rates of ATP hydrolysis recorded over the last 1 min of each assay expressed in μmol of ATP hydrolyzed mg^{-1} min^{-1}.

perchloric acid. Following neutralization of excess acid with KOH, precipitated $KClO_4$ and denatured protein were removed by centrifugation and the supernatants were submitted to anion exchange HPLC to determine enzyme-bound [^{3}H]ADP and [^{3}H]ATP. Radioactivity was determined by liquid scintillation counting in Ecoscint obtained from National Diagnostics.

ATPase activity under multisite conditions was carried out at pH 8.0 and 30 °C using an ATP regeneration system coupled to oxidation of NADH that was determined spectrophotometrically at 340 nm with a Uvikon-XL double-beam spectrophotometer (*15*). Unless stated otherwise, the Mg^{2+} concentration in the assay medium was 1 mM in excess of the ATP concentration.

Fluorescence Titrations of Catalytic Sites of the $\beta Y^{345}W$, $\beta G^{156}C/Y^{345}W$, $\beta E^{199}V/Y^{345}W$, and $\beta G^{156}C/E^{199}V/Y^{345}W$ Mutant Subcomplexes. Titrations of the fluorescence of the introduced tryptophans in the $\beta Y^{345}W$, $\beta G^{156}C/Y^{345}C$, $\beta E^{199}V/Y^{345}W$, and $\beta G^{156}C/E^{199}V/Y^{345}W$ mutant subcomplexes with ADP or ATP in the presence and absence of Mg^{2+} were performed with a Spex Fluoromax-2 spectrofluorometer with excitation at 295 nm and emission at 353 nm. In titrations with MgATP or MgADP, small volumes of solutions of the nucleotides were added to 3 mL of 50 nM $\beta Y^{345}W$, $\beta G^{156}C/Y^{345}W$, $\beta E^{199}V/Y^{345}W$, or $\beta G^{156}C/E^{199}V/Y^{345}W$ mutant subcomplex in 50 mM Tris−Cl, pH 8.0, containing 1 mM $MgCl_2$ in excess of the final concentration of nucleotide. Titrations with ATP or ADP in the absence of $MgCl_2$ were performed under the same conditions in buffer containing 0.1 mM EDTA. Fluorescence quenching was recorded 10 s after addition of nucleotides. In titrations with MgATP, fresh solutions of enzyme were used for each nucleotide concentration examined.

RESULTS

Comparison of the Effects of NaN_3 and LDAO on the Hydrolysis of 2 mM ATP by the Wild-Type, $\beta G^{156}C$, $\beta E^{199}V$, and $\beta G^{156}C/E^{199}V$ Mutant Enzyme Subcomplexes. Figure 1 compares the effects of azide and LDAO on the rate of hydrolysis of 2 mM ATP by the wild-type and mutant enzyme subcomplexes in the presence of an ATP regenerating system. In the absence of additions, the wild-type $\alpha_3\beta_3\gamma$ subcomplex hydrolyzes 2 mM ATP with a specific activity of 20 μmol of ATP hydrolyzed mg^{-1} min^{-1}. Hydrolysis of 2 mM ATP by the wild type is very sensitive to turnover-dependent inhibition by 1 mM NaN_3 and is stimulated 4-fold by 0.06% LDAO. The $\alpha_3(\beta G^{156}C)_3\gamma$ and $\alpha_3(\beta E^{199}V)_3\gamma$ single mutant subcomplexes, in the absence of additions, hydrolyze 2 mM ATP at 2% and 0.7%, respectively, of the rate exhibited by the wild type. In contrast, the $\alpha_3(\beta G^{156}C/E^{199}V)_3\gamma$ double mutant subcomplex, which has higher specific activity than both single mutants, hydrolyzes 2 mM ATP at 9% of the rate exhibited by the wild type. Whereas the steady-state rates of hydrolysis of 2 mM ATP by the wild-type and $\beta E^{199}V$ single mutant enzymes are nearly completely inhibited in the presence of 1 mM NaN_3, the $\beta G^{156}C$ single mutant and $\beta G^{156}C/E^{199}V$ double mutant are inhibited by 9% and 17%, respectively, in the presence of 1 mM NaN_3. Compared to the wild type and $\beta E^{199}V$ single mutant, which are stimulated 4-fold and 5-fold, respectively, in the presence of 0.06% LDAO, the $\beta G^{156}C$ single mutant is stimulated only 1.2-fold under the same conditions. In contrast, the $\beta G^{156}C/E^{199}V$ double mutant is inhibited by 40% in the presence of 0.06% LDAO.

Comparison of the Effects of NaN_3 and LDAO on the Hydrolysis of 2 mM ATP by the $\beta Y^{345}W$, $\beta G^{156}C/Y^{345}W$, $\beta E^{199}V/Y^{345}W$, and $\beta G^{156}C/E^{199}V/Y^{345}W$ Mutant Subcomplexes. Figure 2 compares the effects of NaN_3 and LDAO on the rate of hydrolysis of 2 mM ATP by the $\beta Y^{345}W$ mutant subcomplexes. The $\alpha_3(\beta Y^{345}W)_3\gamma$ single mutant enzyme, which hydrolyzes 2 mM ATP with a specific activity of 24 μmol of ATP hydrolyzed mg^{-1} min^{-1} in the absence of additions, is much less sensitive than the wild type to turnover-dependent inhibition by NaN_3 and is stimulated only 2-fold by 0.06% LDAO. The $\beta E^{199}V/Y^{345}W$ double mutant, which has a higher specific activity than the $\beta E^{199}V$ single mutant, hydrolyzes 2 mM ATP at 1.25% of the rate exhibited by the wild type. Similar to that of the $\beta Y^{345}W$ single mutant, the steady-state rate of ATP hydrolysis by the $\beta E^{199}V/Y^{345}W$ double mutant is less sensitive to azide inhibition as compared to the wild type and $\beta E^{199}V$ single mutant and is stimulated 2-fold by LDAO. In the absence of additions, the $\alpha_3(\beta G^{156}C/Y^{345}W)_3\gamma$ double and $\alpha_3(\beta G^{156}C/E^{199}V/Y^{345}W)_3\gamma$ triple mutant subcomplexes hy-

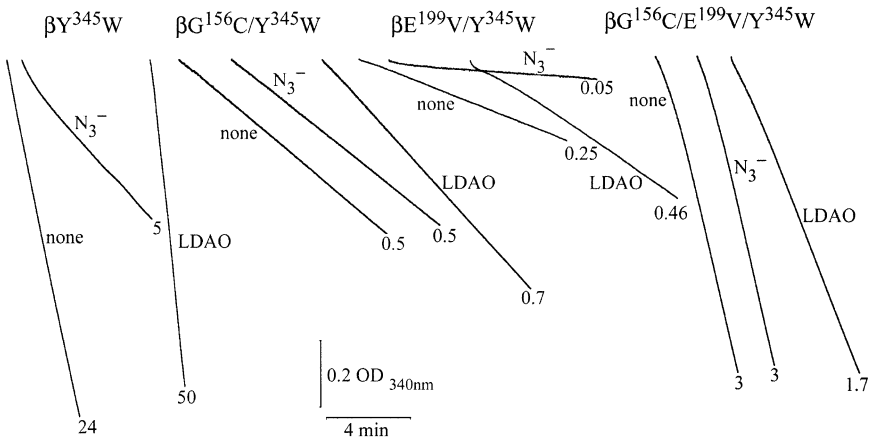

FIGURE 2: Comparison of the effects of NaN_3 and LDAO on the hydrolysis of ATP by the $\beta Y^{345}W$-substituted mutant enzyme subcomplexes. Hydrolysis of 2 mM ATP was carried out as described in the caption of Figure 1. Assays were initiated by injecting 2 μg of the $\beta Y^{345}W$ single mutant or 15 μg each of the $\beta G^{156}C/Y^{345}W$, $\beta E^{199}V/Y^{345}W$, or $\beta G^{156}C/E^{199}V/Y^{345}W$ mutant enzyme subcomplex into 1 mL of assay medium in the presence or absence of 1 mM NaN_3 or 0.06% LDAO, as specified. The numbers on the traces represent the final rates of ATP hydrolysis recorded over the last 1 min of each assay expressed in μmol of ATP hydrolyzed mg^{-1} min^{-1}.

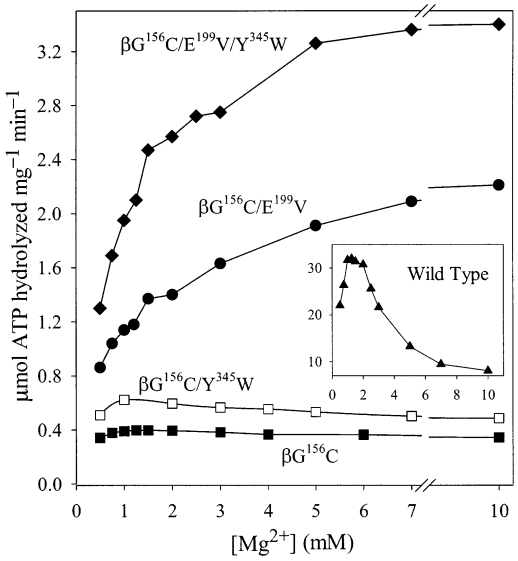

FIGURE 3: Comparison of the effects of increasing Mg^{2+} concentration on the ATPase activity of the wild-type and mutant subcomplexes. A 5 μg sample of the wild type (inset) and 15 μg each of the $\beta G^{156}C$ (closed squares) single mutant, $\beta G^{156}C/Y^{345}W$ (open squares) double mutant, $\beta G^{156}C/E^{199}V$ (closed circles) double mutant, and $\beta G^{156}C/E^{199}V/Y^{345}W$ (closed tilted squares) triple mutant subcomplexes were assayed with the specified concentrations of Mg^{2+} in the presence of 2 mM ATP.

drolyze 2 mM ATP at 2.5% and 15% of the rate exhibited by the wild type. Figure 2 shows that hydrolysis of 2 mM ATP by both the $\beta G^{156}C/Y^{345}W$ double and $\beta G^{156}C/E^{199}V/Y^{345}W$ triple mutant enzymes is insensitive to turnover-dependent inhibition by 1 mM NaN_3. The rate of hydrolysis of ATP by the $\beta G^{156}C/Y^{345}W$ double mutant is stimulated 1.4-fold by 0.06% LDAO, whereas LDAO inhibits the $\beta G^{156}C/E^{199}V/Y^{345}W$ triple mutant by 40%.

Comparison of the Effects of Increasing Concentration of Mg^{2+} on Hydrolysis of 2 mM ATP by the Wild-Type and Mutant Subcomplexes. Figure 3 compares the effects of increasing Mg^{2+} concentration on the rate of hydrolysis catalyzed by the wild-type enzyme (inset, closed triangles) and the $\beta G^{156}C$ single mutant (closed squares), $\beta G^{156}C/Y^{345}W$ double mutant (open squares), $\beta G^{156}C/E^{199}V$ double mutant (closed circles), and $\beta G^{156}C/E^{199}V/Y^{345}W$ triple mutant (closed tilted squares) enzymes. Whereas hydrolysis of 2 mM ATP by the wild-type enzyme becomes increasingly inhibited as the ratio Mg^{2+}/ATP rises above 0.75/1, hydrolysis of 2 mM ATP by the $\beta G^{156}C$ and $\beta G^{156}C/Y^{345}W$ mutants is not inhibited or only slightly inhibited, respectively, when the ratio Mg^{2+}/ATP rises above 1/1. In contrast, hydrolysis of 2 mM ATP by the $\beta G^{156}C/E^{199}V$ double and $\beta G^{156}C/E^{199}V/Y^{345}W$ triple mutant enzymes is stimulated in small increments as the ratio Mg^{2+}/ATP rises above 1/1. The double and triple mutants were stimulated 2-fold and 1.3-fold, respectively, when the ratio was 5/1.

Comparison of the Hydrolysis of Substoichiometric ATP by the Wild-Type and Mutant Subcomplexes. Figure 4A shows that the wild-type (closed circles), $\beta G^{156}C$ (times signs), $\beta G^{156}C/Y^{345}W$ (open triangles), $\beta E^{199}V$ (open squares), $\beta E^{199}V/Y^{345}W$ (closed squares), $\beta G^{156}C/E^{199}V$ (open circles), and $\beta G^{156}C/E^{199}V/Y^{345}W$ (closed triangles) subcomplexes hydrolyze more than 85% of the substoichiometric [^{3}H]ATP added to them within 10 s of mixing. In contrast, the $\beta Y^{345}W$ mutant enzyme (open tilted squares) hydrolyzes substoichiometric [^{3}H]ATP more slowly than the wild type.

Figure 4B shows that product [^{3}H]ADP was not released when the wild-type $\alpha_3\beta_3\gamma$ subcomplex (closed circles) hydrolyzed substoichiometric [^{3}H]ATP. In these experiments, samples of the reaction mixtures were withdrawn at the times indicated and passed through centrifuge columns of Sephadex G-50 directly into centrifuge tubes containing perchloric acid as described by Grubmeyer et al. (*28*). The $\beta Y^{345}W$ (open tilted squares), $\beta E^{199}V$ (open squares), and $\beta E^{199}V/Y^{345}W$ (closed squares) mutant subcomplexes also retained more than 90% of product [^{3}H]ADP after samples of reaction mixtures were passed through centrifuge columns of Sephadex G-50. When submitted to the same procedure, the $\beta G^{156}C$ subcomplex (times signs) did not retain bound [^{3}H]ADP and the $\beta G^{156}C/Y^{345}W$ subcomplex (open triangles) retained about 20% of product [^{3}H]ADP after greater than 90% of the added [^{3}H]ATP was hydrolyzed. In the case of the $\beta G^{156}C/E^{199}V$ double mutant (open circles), about 55% of the product [^{3}H]ADP remained bound to the enzyme after samples of the reaction mixture were passed through centrifuge columns of Sephadex G-50. The $\beta G^{156}C/E^{199}V/Y^{345}W$ (closed triangles) triple mutant retained about 60%

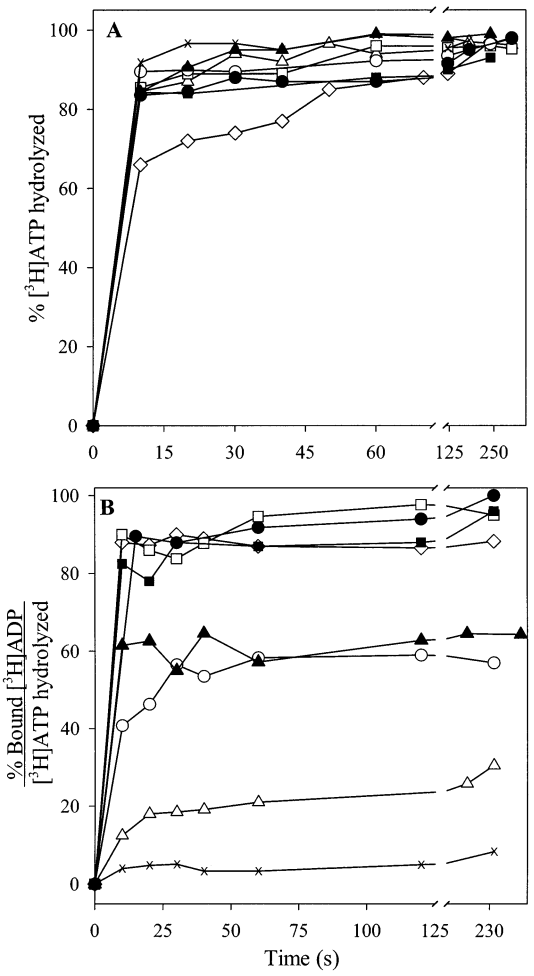

FIGURE 4: Hydrolysis of substoichiometric [^{3}H]ATP by the wild-type and mutant subcomplexes. A 2.85 μM sample of the wild type (closed circles) and $\beta Y^{345}W$ (open tilted squares), $\beta E^{199}V$ (open squares), $\beta G^{156}C$ (times signs), $\beta G^{156}C/Y^{345}W$ (open triangles), $\beta G^{156}C/E^{199}V$ (open circles), $\beta E^{199}V/Y^{345}W$ (closed squares), and $\beta G^{156}C/E^{199}V/Y^{345}W$ (closed triangles) mutant enzymes were rapidly mixed with [^{3}H]ATP added to a final concentration of 1.7 μM at 23 °C in 50 mM Tris−Cl, pH 8.0, containing 1 mM Mg^{2+}. The reactions were either quenched at the specified times by addition of perchloric acid (A) or passed through 1 mL centrifuge columns of Sephadex G-50 prior to quenching with perchloric acid (B), as described in the Experimental Procedures.

of product [^{3}H]ADP under the same experimental conditions.

Comparison of the Affinities of Catalytic Sites in the $\beta Y^{345}W$, $\beta G^{156}C/Y^{345}W$, $\beta E^{199}V/Y^{345}W$, and $\beta G^{156}C/E^{199}V/Y^{345}W$ Mutant Enzymes for Nucleotides. Figure 5 compares fluorescence titrations of the $\beta Y^{345}W$ single mutant (circles), $\beta G^{156}C/Y^{345}W$ (triangles) and $\beta E^{199}V/Y^{345}W$ (tilted squares) double mutants, and $\beta G^{156}C/E^{199}V/Y^{345}W$ triple mutant (squares) with ADP or ATP in the presence and absence of Mg^{2+}. In titrations of the $\beta Y^{345}W$ single mutant with MgADP and MgATP illustrated in parts A and B, respectively, of Figure 5, all of the ADP or ATP was bound until the molar ratio of added nucleotide over enzyme was greater than 1.7/1. Therefore, it was not possible to determine K_{d1} and K_{d2} values for MgADP or MgATP binding to catalytic sites 1 and 2 for this mutant. In contrast, it was possible to estimate three K_d values when the $\beta G^{156}C/Y^{345}W$ double mutant and $\beta G^{156}C/E^{199}V/Y^{345}W$ triple mutant were titrated with ADP or ATP in the presence of Mg^{2+}. Solid lines represent the best-fit theoretical curves generated on the basis of experimental data for titrations with ATP and ADP in the presence and absence of Mg^{2+} assuming three catalytic sites with different binding affinities. Dashed lines in Figure 5C,D represent theoretical curves generated on the basis of the experimental data assuming three catalytic sites with identical affinity for ADP or ATP in the absence of Mg^{2+}. Clearly, the experimental data do not fit this model. The K_d values estimated from the titration curves illustrated by solid lines using the equation described by Weber et al. (*29*) are summarized in Table 1.

It is clear from the K_d values listed in Table 1 that all three catalytic sites in the $\beta G^{156}C/Y^{345}W$ double mutant have considerably lower affinity for MgADP and MgATP than the $\beta Y^{345}W$ single mutant. The comparison of the K_d values obtained for ADP and ATP binding to catalytic sites of the $\beta Y^{345}W$ single mutant and $\beta G^{156}C/Y^{345}W$ double mutant listed in Table 1 provides a comprehensive evaluation of the effects of the $\beta G^{156}C$ substitution on the affinities of the three catalytic sites for nucleotides. The affinities of catalytic sites 1, 2, and 3 for ADP in the absence of Mg^{2+} are about 22-fold, 12-fold, and 12-fold lower, respectively, in the $\beta G^{156}C/Y^{345}W$ double mutant than in the $\beta Y^{345}W$ single mutant. In the case of ATP binding in the absence of Mg^{2+}, the $\beta G^{156}C$ substitution decreases the affinities of catalytic sites 1, 2, and 3 by about 1000-fold, 18-fold, and 17-fold, respectively. The K_d values summarized in Table 1 also clearly indicate that all three catalytic sites in the $\beta G^{156}C/Y^{345}W$ double mutant have considerably higher affinity for ADP than ATP in the absence of Mg^{2+}.

The K_d values summarized in Table 1 indicate that insertion of the $\beta E^{199}V$ substitution into either the $\beta Y^{345}W$ single or $\beta G^{156}C/Y^{345}W$ double mutant increases the affinities of catalytic sites for nucleotides. The $\beta E^{199}V/Y^{345}W$ double mutant shows 20-fold and 16-fold higher affinities in catalytic site 3 for MgADP and MgATP, respectively, than the $\beta Y^{345}W$ single mutant. In the absence of Mg^{2+}, the affinities of all three catalytic sites of the $\beta E^{199}V/Y^{345}W$ double mutant for ADP or ATP are considerably higher than those exhibited by the $\beta Y^{345}W$ mutant. The affinities of catalytic sites 1, 2, and 3 for MgADP in the $\beta G^{156}C/E^{199}V/Y^{345}W$ triple mutant are 6-fold, 37-fold, and 38-fold higher, respectively, than those observed with the $\beta G^{156}C/Y^{345}W$ double mutant. The affinities of all three catalytic sites for MgATP are also considerably higher in the $\beta G^{156}C/E^{199}V/Y^{345}W$ triple mutant than in the $\beta G^{156}C/Y^{345}W$ double mutant. It is interesting that the K_{d1} and K_{d2} values obtained with the $\beta G^{156}C/E^{199}V/Y^{345}W$ triple mutant for both MgADP and MgATP are higher than those obtained with the $\beta Y^{345}W$ single mutant, whereas the K_{d3} values for both MgADP and MgATP are considerably lower in the triple mutant than the K_{d3} values obtained with the $\beta Y^{345}W$ single mutant.

The $\alpha_3(\beta G^{156}C)_3\gamma$ Subcomplex Hydrolyzes ATP Noncooperatively. Figure 6 compares Lineweaver−Burk plots constructed from the rates of hydrolysis of 8−2000 μM ATP by the $\beta G^{156}C$ single mutant (open circles), $\beta G^{156}C/E^{199}V$ double mutant (open triangles), $\beta G^{156}C/E^{199}V/Y^{345}W$ triple mutant (open squares), and wild-type subcomplex in the presence of LDAO (closed circles). Lineweaver−Burk plots obtained with the $\beta G^{156}C/E^{199}V$ double mutant and the $\beta G^{156}C/E^{199}V/Y^{345}W$ triple mutant, like that of the wild-type enzyme in the presence of LDAO, are linear. In contrast, the reciprocal plot obtained with the $\beta G^{156}C$ single mutant

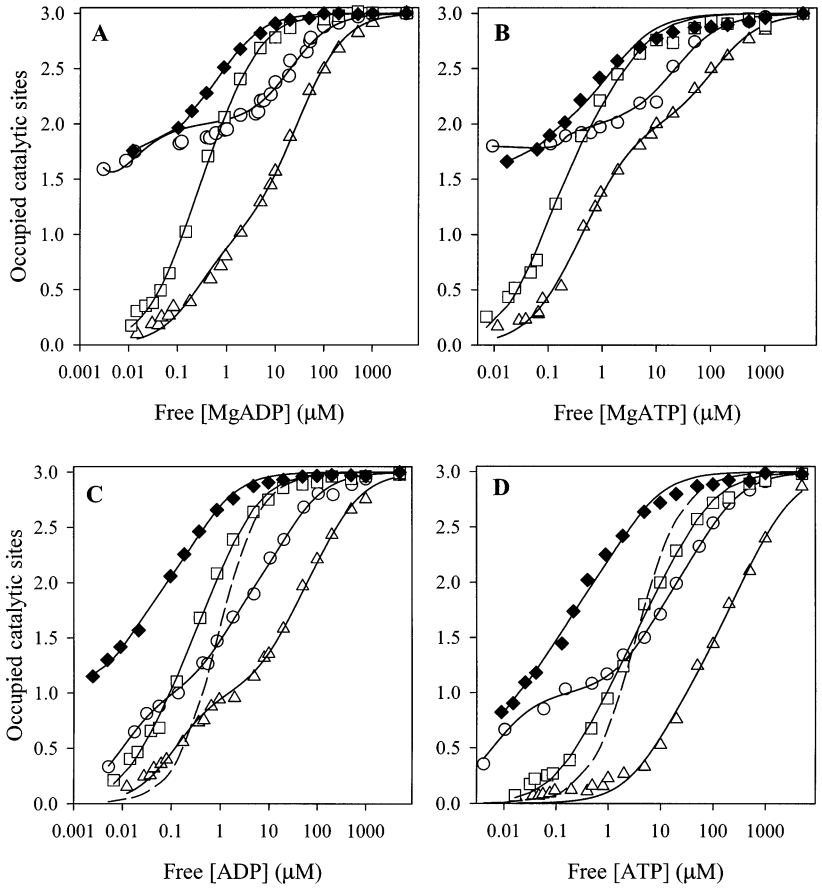

FIGURE 5: Fluorescence titrations of the introduced tryptophans in the $\beta Y^{345}W$, $\beta G^{156}C/Y^{345}W$, $\beta E^{199}V/Y^{345}W$, and $\beta G^{156}C/E^{199}V/Y^{345}W$ mutant enzyme subcomplexes with ADP and ATP in the presence and absence of Mg^{2+}: (A) titration with MgADP, (B) titration with MgATP, (C) titration with ADP, (D) titration with ATP. Fluorescence measurements with the $\beta Y^{345}W$ (open circles), $\beta G^{156}C/Y^{345}W$ (open triangles), $\beta E^{199}V/Y^{345}W$ (closed tilted squares), and $\beta G^{156}C/E^{199}V/Y^{345}W$ (open squares) mutant enzyme subcomplexes were performed as described in the Experimental Procedure. Concentrations of free nucleotides were obtained at each data point by subtracting the amount of bound nucleotide determined from quenching from the total concentration of nucleotide in the reaction mixture. Solid lines were obtained from nonlinear regression analysis of the experimental data using an equation assuming three independent binding sites described by Weber et al. (*29*). Dashed lines in (C) and (D) represent nonlinear regression analyses of the experimental data obtained from titrations of the $\beta Y^{345}W$ single mutant with ADP or ATP, respectively, assuming three catalytic sites of equal affinity in the absence of Mg^{2+}.

Table 1: Comparison of the K_d Values (μM) Obtained from Fluorescence Titrations of the $\alpha_3(\beta Y^{345}W)_3\gamma$, $\alpha_3(\beta G^{156}C/Y^{345}W)_3\gamma$, $\alpha_3(\beta E^{199}V/Y^{345}W)_3\gamma$, and $\alpha_3(\beta G^{156}C/E^{199}V/Y^{345}W)_3\gamma$ Mutant Subcomplexes with Nucleotides

	dissociation constant	$\beta Y^{345}W$	$\beta G^{156}C/Y^{345}W$	$\beta G^{156}C/E^{199}V/Y^{345}W$	$\beta E^{199}V/Y^{345}W$
MgADP	K_{d1}	*a*	0.28 (±0.02)	0.045 (±0.007)	*a*
	K_{d2}	*a*	11 (±3.2)	0.3	*a*
	K_{d3}	20 (±2.0)	90 (±14)	2.3 (±0.5)	1.0 (±0.05)
MgATP	K_{d1}	*a*	0.22 (±0.05)	0.025 (±0.007)	*a*
	K_{d2}	*a*	1.03 (±0.05)	0.25 (±0.007)	*a*
	K_{d3}	24 (±1.7)	120 (±10)	3	1.5 (±0.02)
ADP	K_{d1}	0.01 (±0.004)	0.22 (±0.10)	0.028 (±0.008)	*a*
	K_{d2}	1.6 (±0.5)	20 (±0.5)	0.26 (±0.03)	0.021 (±0.004)
	K_{d3}	27 (±2.8)	315 (±35)	3	0.5 (±0.07)
ATP	K_{d1}	0.01 (±0.003)	10.5 (±2.1)	0.27 (±0.03)	*a*
	K_{d2}	8 (±3)	149 (±38)	3	0.13 (±0.02)
	K_{d3}	74 (±2.3)	1285 (±120)	40	2.3 (±0.1)

[a] The K_d value was too low to determine using the method described in the caption of Figure 5.

is curved concave downward. A nonlinear Lineweaver−Burk plot was also obtained when the $\beta G^{156}C$ mutant enzyme hydrolyzed 8−2000 μM ATP in the presence of 0.06% LDAO.

A K_m value of 43 μM and a k_{cat} value of 423 s^{-1} were obtained from the Lineweaver−Burk plot for the wild-type subcomplex illustrated in Figure 6 that was determined in the presence of 0.06% LDAO. Magnification of the Lineweaver−Burk plot for the $\beta G^{156}C$ mutant subcomplex illustrated in Figure 6, over the limited 500−2000 μM ATP concentration range, revealed a linear plot with intercepts corresponding to K_m and k_{cat} values of 80 μM and 1.7 s^{-1}, respectively. Taking into account the K_d values for binding nucleotides to catalytic sites of the $\beta G^{156}C/Y^{345}W$ mutant given in Table 1, it is reasonable to assume that the extrapolated K_m and k_{cat} values obtained with the $\beta G^{156}C$

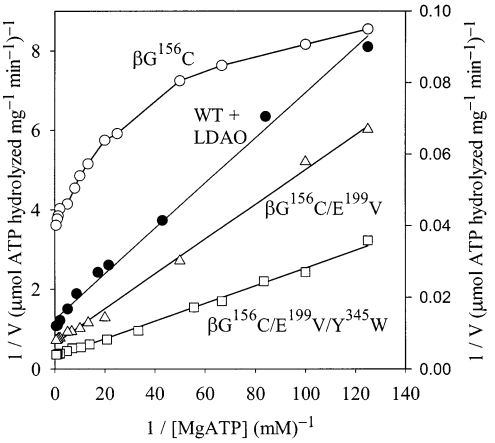

FIGURE 6: Lineweaver−Burk plots for ATP hydrolysis by the wild-type and $\beta G^{156}C$, $\beta G^{156}C/E^{199}V$, and $\beta G^{156}C/E^{199}V/Y^{345}W$ mutant subcomplexes. Hydrolysis of 8−2000 μM ATP by the $\beta G^{156}C$ single mutant (open circles), $\beta G^{156}C/E^{199}V$ double mutant (open triangles), and $\beta G^{156}C/E^{199}V/Y^{345}W$ triple mutant (open squares) was conducted as described in the Experimental Procedures in the presence of 1 mM excess Mg^{2+} over the ATP concentrations. Hydrolysis of 8−2000 μM ATP by the wild type in the presence of 0.06% LDAO (closed circles) was carried out under the same conditions (plotted with a different scale on the right *y*-axis).

mutant over the limited ATP concentration range are associated with saturation of the third catalytic site. If this is indeed the case, the deviations from linearity observed in the plot at lower ATP concentrations would be due to ATP hydrolysis at catalytic sites 1 and 2 acting independently, each with its own K_m and k_{cat} values.

To test this possibility, the rates of hydrolysis of 1, 2, and 10 μM ATP were determined with the $\beta G^{156}C$, $\beta G^{156}C/E^{199}V$, and $\beta G^{156}C/E^{199}V/Y^{345}W$ mutant subcomplexes in the absence of LDAO and with the wild-type subcomplex in the presence of LDAO. The rate observed at each ATP concentration was compared with the rate calculated using the K_m and k_{cat} values determined from the Lineweaver−Burk plots illustrated in Figure 6. The results of these comparisons are summarized in Table 2. The experimentally determined rates of hydrolysis of 1, 2, and 10 μM ATP by the $\beta G^{156}C$ mutant enzyme are 20-fold, 10-fold, and 4-fold greater than the rates calculated from the K_m and k_{cat} values extrapolated from the straight line portion (500−2000 μM ATP) of the expanded version of the Lineweaver−Burk plot illustrated in Figure 6. The observation that deviation between the observed rate and the calculated rate decreases with increasing ATP concentration is consistent with the premise that the three catalytic sites of the $\beta G^{156}C$ mutant subcomplex hydrolyze ATP independently, each with its own K_m and k_{cat} values. This is responsible for the downward curvature of the Lineweaver−Burk plot for this mutant enzyme illustrated in Figure 6 as the ATP concentration decreases below 500 μM. In contrast, the experimentally determined rates of hydrolysis of the same low concentrations of ATP observed with the wild-type enzyme in the presence of LDAO and the $\beta G^{156}C/E^{199}V$ and $\beta G^{156}C/E^{199}V/Y^{345}W$ mutants in the absence of LDAO closely agree with the rates calculated from the K_m and k_{cat} values extrapolated from the linear Lineweaver−Burk plots illustrated in Figure 6. Since single-molecule studies have shown that the three catalytic sites of the wild-type subcomplex fire one at a time in a highly cooperative sequence (*7*−*9*), the linear Lineweaver−Burk plots exhibited by the $\beta G^{156}C/E^{199}V$ and $\beta G^{156}C/E^{199}V/Y^{345}W$ mutant subcomplexes show that insertion of the $\beta E^{199}V$ substitution into the $\beta G^{156}C$ and $\beta G^{156}C/Y^{345}W$ mutants restores cooperative, sequential firing of catalytic sites.

It is curious that the experimentally determined K_m value for the $\beta G^{156}C/E^{199}V/Y^{345}W$ triple mutant of 69 μM (Table 2) is significantly lower than the K_{d3} value of 3 μM determined in the fluorescence titration of the enzyme with MgATP (Table 1). Whereas the steady-state kinetic analysis was performed in the presence of an ATP regenerating system, product MgADP accumulated in each reaction mixture examined in the fluorescence titration with MgATP in the absence of ATP regeneration. This may be responsible for the discrepancy.

DISCUSSION

Comparison of fluorescence titrations of introduced tryptophans in the $\beta Y^{345}W$ single mutant and the $\beta G^{156}C/Y^{345}W$ double mutant with ADP and ATP in the presence or absence of Mg^{2+} clearly shows that the $\beta G^{156}C$ substitution in the $\alpha_3\beta_3\gamma$ subcomplex substantially decreases the affinity of catalytic sites for nucleotides. This is consistent with the observation that the $\beta G^{156}C$ and $\beta G^{156}C/ Y^{345}W$ mutant enzymes release product [^{3}H]ADP when they hydrolyze substoichiometric [^{3}H]ATP, whereas product [^{3}H]ADP remains tightly bound when the wild-type and $\beta Y^{345}W$ mutant enzymes hydrolyze substoichiometric [^{3}H]ATP. Therefore, it is clear that the $\beta G^{156}C$ substitution distorts the Ω-loop in β subunits comprised of residues ^{156}GGAGVG^{161} in a manner that destabilizes the closed conformation of the catalytic site. It is interesting that the $\beta G^{156}C/E^{199}V$ double mutant hydrolyzes 2 mM ATP at 9% of the rate exhibited by the wild-type enzyme, whereas the $\beta G^{156}C$ and $\beta E^{199}V$ single mutant enzymes hydrolyze 2 mM ATP at 2% and 0.7%, respectively, of the rate exhibited by the wild-type enzyme. It appears that insertion of the $\beta E^{199}V$ substitution into the $\beta G^{156}C$ mutant enzyme partly restores ATPase activity by

Table 2: Comparison of the Observed Rates of Hydrolysis of Low ATP Concentrations with Rates Calculated from the K_m and k_{cat} Values Extrapolated from the Lineweaver−Burk Plots in Figure 6[a]

			v at 1 μM ATP		*v* at 2 μM ATP		*v* at 10 μM ATP	
enzyme	k_{cat} (s^{-1})	K_m (μM)	obsd	calcd	obsd	calcd	obsd	calcd
wild type + LDAO	423	43	13	10	22	19	76	80
$\beta G^{156}C$	1.7	80	0.4	0.02	0.5	0.04	0.8	0.2
$\beta G^{156}C/E^{199}V$	9	66	0.3	0.2	0.4	0.3	1.7	1.3
$\beta G^{156}C/E^{199}V/Y^{345}W$	19	69	0.4	0.3	0.5	0.5	2.0	2.4

[a] Assays were initiated by injecting of 5 mg of the wild type or 15 mg of the mutant subcomplexes into 1 mL of assay medium (*15*) containing 1 M excess $MgCl_2$ over the final concentrations of ATP. The wild-type subcomplex was assayed in the presence of 0.06% LDAO. The observed rates are the average of three determinations. The rates, *v*, are in (mol of ATP hydrolyzed/mol of subcomplex)/s.

restabilizing the closed conformation of catalytic sites without restoring sensitivity to inhibition by azide.

By correlating catalytic site occupancy of the $\beta Y^{345}W$ mutant of EF_1, established by fluorescence quenching of the introduced tryptophans, with the dependence of ATPase activity on ATP concentration, Weber et al. (*29*) established that significant rates of hydrolysis do not occur until MgATP binds to the catalytic site of lowest affinity. The same correlation was established when the $\alpha_3(\beta Y^{345}W)_3\gamma$ subcomplex of TF_1 was examined in the presence of 0.06% LDAO (*25*). Therefore, the linear Lineweaver−Burk plot obtained with the wild-type enzyme in the presence of LDAO represents cooperative, trisite ATP hydrolysis. From the analysis described in detail in the Results, the curved Lineweaver−Burk plot obtained with the $\beta G^{156}C$ mutant enzyme deviates from linearity in a manner indicating that it hydrolyzes ATP in the absence of cooperative interactions between catalytic sites. In contrast, the Lineweaver−Burk plots obtained with the $\beta G^{156}C/ E^{199}V$ double mutant and $\beta G^{156}C/E^{199}V/Y^{345}W$ triple mutant enzymes are linear. Therefore, insertion of the $\beta E^{199}V$ substitution into the $\beta G^{156}C$ single mutant or $\beta G^{156}C/Y^{345}W$ double mutant restores cooperativity between catalytic sites. This is consistent with the observation that product [^{3}H]ADP is retained, albeit less firmly than with the wild type, when the $\beta G^{156}C/E^{199}V$ and $\beta G^{156}C/E^{199}V/Y^{345}W$ mutant enzymes hydrolyze [^{3}H]ATP at a single catalytic site. Furthermore, restoration of cooperativity between catalytic sites by insertion of the $\beta E^{199}V$ substitution into the $\beta G^{156}C$ mutant of the *E. coli* ATP synthase is probably responsible for the observation that an *E. coli* strain carrying the double substitution grows on succinate, whereas the strain carrying the $\beta G^{156}C$ single substitution does not grow on succinate (*22*).

Yoshida et al. have proposed a trisite model to explain the 90° and 30° substeps observed in rotation of the γ subunit when single molecules of the $\alpha_3\beta_3\gamma$ subcomplex of TF_1 hydrolyze ATP (*2*). The reaction cycle illustrated in Figure 7 illustrates a variation of their model that takes into account the results presented here which suggest that formation of the transition state is part of the cooperative process that governs sequential firing of catalytic sites. In the initial CCO state, two β subunits are in closed conformations (C) containing MgATP in closed catalytic sites. The third β subunit, containing an open catalytic site, has an open conformation (O). The reaction cycle is initiated when MgATP binds to the empty catalytic site. This is accompanied by three events: (1) the γ subunit rotates 90° in the counterclockwise direction, (2) the open catalytic site converts to a partly closed conformation (C′), and (3) the adjacent β subunit converts to a partly open conformation (C″) in which amino acid side chains are now arranged appropriately to form the transition state [ATP]. The curved arrow represents transmission of a signal from the catalytic site that is in the process of closing upon binding MgATP to the catalytic site that forms the transition state as it opens. The reaction cycle is completed when products dissociate from the latter site. This is accompanied by rotation of the γ subunit through an additional 30° in the counterclockwise direction, thus resetting the enzyme for another round of rotational catalysis.

The major feature that distinguishes the model illustrated in Figure 7 from the model proposed by Yoshida et al. (*2*)

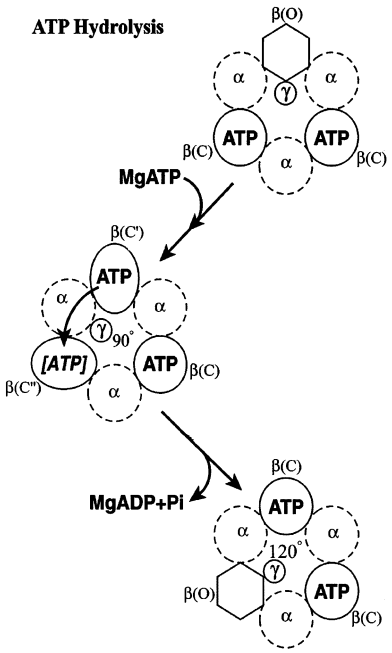

FIGURE 7: A model for a single round of rotary ATP hydrolysis: circles with dashed-lines, α subunits liganded with MgATP; circles with solid lines, β subunits liganded with MgATP; hexagons, empty and open β subunits; ellipses, β subunits that are in transition from the open to closed conformation. [ATP] represents the transition state for ATP hydrolysis.

is our contention that the transition state forms when a catalytic site containing tightly bound MgATP converts from the closed conformation to the open conformation (*30*). This contention is supported by the results presented which indicate that the $\beta G^{156}C$ substitution distorts the Ω-loop in catalytic sites in a manner that allows formation of the transition state in the absence of cooperative interactions between catalytic sites. However, in the absence of definitive structural information, other interpretations of the aberrant catalytic properties of the $\alpha_3(\beta G^{156}C)_3\gamma$ subcomplex are possible.

That both the $\beta G^{156}C$ single mutant and $\beta G^{156}C/Y^{345}W$ double mutant have much lower sensitivity to inhibition by azide than the wild type is consistent with the low sensitivity of the $\beta G^{156}S$ mutant of EF_1 to inhibition by azide reported by Iwamoto et al. (*31*). Moreover, they also reported that the $\beta G^{156}S$ mutant of EF_1 has altered specificity for divalent metal ions, indicating a connection between azide inhibition and the divalent metal ion complexed with bound nucleotides. Consistent with this argument, it has been shown that azide stabilizes the dead end Mn^{2+}−ADP−creatine complex bound to the active site of creatine kinase by coordinating with the Mn^{2+} (*32*). Therefore, to explain the lowered sensitivity to inhibition by azide, it is possible that the substitution of βGly^{156} with Cys or Ser alters the orientation of the Mg^{2+} ion complexed with ADP at the catalytic site in a manner that reduces its susceptibility to coordinate with N_3^-.

It is interesting that the ATPase activity of the $\alpha_3(\beta F^{155}W)_3\gamma$ subcomplex of TF_1 resembles that of the $\beta G^{156}C$ mutant subcomplex in that it has decreased sensitivity to inhibition by azide compared to the wild-type enzyme and is not inhibited by free Mg^{2+} ion in the assay medium (*33*). However, the specific ATPase activity of the $\beta F^{155}W$ mutant is about 3-fold greater than that of the wild-type enzyme, whereas the specific activity of the $\beta G^{156}C$ mutant is only

2% that of the wild-type enzyme. The $\beta F^{155}W$ mutant subcomplex binds [^{3}H]ADP in the presence of Mg^{2+} with high affinity. It has been shown that, after treatment with stoichiometric [^{3}H]ADP in the presence of 1 mM Mg^{2+} followed by passage through a centrifuge column of Sephadex G-50, the $\beta F^{155}W$ mutant subcomplex retains greater than 0.9 mol of [^{3}H]ADP/mol of enzyme (*33*). Therefore, decreased sensitivity to inhibition by azide or excess Mg^{2+} in the assay medium does not necessarily reflect low affinity of catalytic sites for nucleotides.

The finding that three K_d values were obtained for ATP or ADP in the absence of Mg^{2+} in fluorescence titrations of the $\beta Y^{345}W$, $\beta G^{156}C/Y^{345}W$, $\beta E^{199}V/Y^{345}W$, and $\beta G^{156}C/E^{199}V/Y^{345}W$ mutant enzymes conflicts with results of similar titrations of the $\beta Y^{345}W$ mutant of EF_1. Only single K_d values of 76 and 83 μM were observed when the tryptophan fluorescence of the $\beta Y^{345}W$ mutant of EF_1 was titrated with ADP and ATP in the absence of Mg^{2+} (*34*). As pointed out earlier (*33*), this discrepancy is probably caused by the presence of endogenous nucleotides in the EF_1 preparations examined by Weber et al. (*34*). The TF_1 subcomplexes that were submitted to fluorescence titrations in this study were free of endogenous nucleotides.

REFERENCES

1. Boyer, P. D. (1997) *Annu. Rev. Biochem. 66*, 717−749.
2. Yoshida, M., Muneyuki, E., and Hisabori, T. (2001) *Nat. Rev./Mol. Cell Biol. 2*, 669−677.
3. Abrahams, J. P., Leslie, A. G. W., Lutter, R. and Walker, J. E. (1994) *Nature 370*, 621−628.
4. Oriss, G. L., Leslie, A. G. W., Braig, K., and Walker, J. E. (1998) *Structure 6*, 831−837.
5. Gibbons, C., Montgomery, M. G., Leslie, A. G. W., and Walker, J. E. (2000) *Nat. Struct. Biol. 7*, 1055−1061.
6. Menz, R. I., Walker, J. E., and Leslie, A. G. W. (2001) *Cell 106*, 331−341.
7. Noji, H., Yasuda, R., Yoshida, M., and Kinosita, K., Jr. (1997) *Nature 386*, 299−302.
8. Yasuda, R., Noji, H., Kinosita, K., and Yoshida, M. (1998) *Cell 93*, 1117−1124.
9. Yasuda, R., Noji, H., Yoshida, M., Kinosita, K., and Itoh, H. (2001) *Nature 410*, 898−204.
10. Drobinskaya, I. Y., Kozlov, I. A., Murataliev, M. B., and Vulfson, E. N. (1985) *FEBS Lett. 182*, 419−423.
11. Milgrom, Y. M., and Murataliev, M. B. (1989) *Biochim. Biophys. Acta 975*, 50−58.
12. Milgrom, Y. M., and Boyer, P. D. (1990) *Biochim. Biophys. Acta 1020*, 43−48.
13. Chernyak, B. V., and Cross, R. L. (1992) *Arch. Biochem. Biophys. 295*, 247−252.
14. Vasilyeva, E. A., Minkov, I. B., and Vinogradov, A. D. (1982) *Biochem. J. 202*, 9−14.
15. Jault, J.-M., and Allison, W. S. (1993) *J. Biol. Chem. 268*, 1558−1566.
16. Paik, S. R., Jault, J-. M., and Allison, W. S. (1994) *Biochemistry 33*, 126−133.
17. Jault, J.-M., Matsui, T., Jault, F. M., Kaibara, C., Muneyuki, E., Yoshida, M. Ohta, T., Kagawa, Y., and Allison, W. S. (1995) *Biochemistry 34*, 16412−16418.
18. Vasilyeva, E. A., Minkov, I. B., Fitin, A. F., and Vinogradov, A. D. (1982) *Biochem. J. 202*, 15−23.
19. Kalashnikova, T. Y., Milgrom, Y. M., and Murataliev, M. B. (1988) *Eur. J. Biochem. 177*, 213-218.
20. Jault, J-. M, Paik, S. R., Grodsky, N. B., and Allison, W. S. (1994) *Biochemistry 33*, 14979−14985.
21. Ren, H., and Allison, W. S. (2000) *J. Biol. Chem. 275*, 10057−10063.
22. Iwamoto, A., Park, M.-Y, Maeda, M., and Futai, M. (1993) *J. Biol. Chem. 268*, 3156−3160.
23. Leszczynski, J. F., and Rose, G. D. (1986) *Science 234*, 849−855.
24. Matsui, T., and Yoshida, M. (1995) *Biochim. Biophys. Acta 1231*, 139−146.
25. Dou, C., Fortes, P. A. G., and Allison, W. S. (1998) *Biochemistry 37*, 16757-16764.
26. Penefsky, H. S. (1977) *J. Biol. Chem. 252*, 2891−2899.
27. Bradford, M. M. (1976) *Anal. Biochem. 72*, 248−254.
28. Grubmeyer, C., Cross, R. L., and Penefsky, H. S. (1982) *J. Biol. Chem. 257*, 12092−12100.
29. Weber, J., Wilke-Mounts, S., Lee, R. S.-F., Grell, E., and Senior, A. E. (1993) *J. Biol. Chem. 268*, 20126−20133.
30. Allison, W. S., Ren, H., and Dou, C. (2000) *J. Bioenerg. Biomembr. 32*, 531−538.
31. Iwamoto, A., Omote, H., Hanada, H., Nobuo, T., Akiko, I., Maeda, M., and Futai, M. (1991) *J. Biol. Chem. 266*, 16350−16355.
32. Reed, G. H., Barlow, C. H., and Burns, R. A., Jr. (1978) *J. Biol. Chem. 253*, 4153−4158.
33. Dong, K., Ren, H., and Allison, W. S. (2002) *J. Biol. Chem. 277*, 9540−9547.
34. Weber, J., Wilke- Mounts, S., and Senior, A. E. (1994) *J. Biol. Chem. 269*, 20462−20467.

BI026243G